

Correlations in eigenfunctions of quantum chaotic systems with sparse Hamiltonian matrices

Jiaozi Wang and Wen-ge Wang*

Department of Modern Physics, University of Science and Technology of China, Hefei 230026, China

(Received 27 March 2015; revised manuscript received 18 September 2017; published 27 November 2017)

In most realistic models for quantum chaotic systems, the Hamiltonian matrices in unperturbed bases have a sparse structure. We study correlations in eigenfunctions of such systems and derive explicit expressions for some of the correlation functions with respect to energy. The analytical results are tested in several models by numerical simulations. Some applications are discussed for a relation between transition probabilities and for expectation values of some local observables.

DOI: [10.1103/PhysRevE.96.052221](https://doi.org/10.1103/PhysRevE.96.052221)

I. INTRODUCTION

Statistical properties of energy eigenfunctions (EFs) of quantum chaotic systems have been studied extensively in the past years [1–26]. They are of interest in various fields of physics and have many applications, e.g., in statistical and transport properties in chaotic quantum dots [27,28], in wave functions in optical, elastomechanical, and microwave resonators [29–35], and in the decay and fluctuations of heavy nuclei [36–38]. In particular, they play an important role in the understanding of thermalization [39–43].

Due to the remarkable success of the random-matrix theory (RMT) in the description of statistical properties of energy levels of quantum chaotic systems [1–3,44], it would be natural to expect that the RMT may be useful in the description of statistical properties of EFs in these systems. Indeed, this expectation has led to some successful applications (see, e.g., reviews given in Refs. [3,45]). In fact, restricted to main bodies of EFs [5], or to the so-called nonperturbative regions of the EFs [46,47], numerical simulations show that the distribution of the components of the EFs has a Gaussian shape, as predicted by the RMT. But, deviation from the Gaussian distribution has been observed, when the tail regions of EFs are taken into account [6].

Consistently, for EFs in the configuration space, Berry's conjecture assumes uncorrelated phases for their components in the momentum representation [4]. Based on Berry's conjecture and semiclassical analysis, it has been found that neighboring EFs in many-body systems predict similar results for local observables [40]. This property, which has also been found in a RMT study [39], is of relevance to thermalization and, in a broader situation, is nowadays referred to as eigenstates thermalization hypothesis (ETH) [41]. Furthermore, when specific dynamics, e.g., periodic orbits and long-range correlations, are taken into account, modifications should be introduced to Berry's conjecture [10–14].

In fact, for EFs in chaotic many-body quantum systems, correlations more than that predicted by the original RMT have been found and modified versions of the RMT have been investigated [48–51]. For example, contrary to the vanishing correlation function predicted by the RMT, in a many-body system with a sparse Hamiltonian matrix, nonvanishing four-point correlations have been observed, which are of relevance

to important physical quantities such as transition probabilities [8]. Moreover, correlations have been studied for operators at different times in a two-dimensional kicked quantum Ising model [52].

In this paper, we study correlations among components of EFs, particularly the phase correlations, in quantum chaotic systems whose Hamiltonian matrices have a sparse structure in unperturbed bases. Such a sparse structure is commonplace in realistic models. Under this structure, each unperturbed state is coupled to a small fraction of other unperturbed states. As a result, it is reasonable to expect certain correlations among components of the EFs, as shown in the example mentioned above in Ref. [8]. We derive explicit expressions for some of the correlation functions and test the results by numerical simulations. We also discuss some applications of the results.

The paper is organized as follows. In Sec. II, we discuss the models to be employed. Section III is devoted to generic discussions for the type of correlation functions to be studied. Then, some specific correlation functions are discussed in Sec. IV, for the case in which the perturbation matrix has elements with a homogeneous sign. The case with nonhomogeneous signs of the matrix elements is discussed in Sec. V. Some applications are given in Sec. VI for a relation between some transition probabilities, as well as for expectation values of some local observables. Finally, conclusions are given in Sec. VII.

II. MODELS EMPLOYED

We consider quantum chaotic systems, for each of which the Hamiltonian is written as $H = H_0 + V$, where H_0 is an unperturbed Hamiltonian and V indicates a perturbation. We'll employ four models in our numerical simulations. Parameters in the four models are set such that they are in the quantum chaotic regime, in which the distribution of the nearest-level spacings is close to the prediction of the RMT.

The first model we consider is a three-orbital LMG model [53]. This model is composed of Ω particles, occupying three energy levels labeled by $r = 0, 1, 2$, each with Ω degeneracy. Here, we are interested in the collective motion of this model. We use ϵ_r to denote the energy of the r th level and, for brevity, we set $\epsilon_0 = 0$. The Hamiltonian of the model is written as

$$H = H_0 + V, \quad (1)$$

*wgwang@ustc.edu.cn

where H_0 and V are the unperturbed Hamiltonian and the perturbation, respectively,

$$H_0 = \epsilon_1 K_{11} + \epsilon_2 K_{22}, \quad V = \sum_{i=1}^4 \mu_i V^{(i)}. \quad (2)$$

Here, K_{rr} represents the particle number operator for the level r and

$$V^{(1)} = K_{10}K_{10} + K_{01}K_{01}, \quad V^{(2)} = K_{20}K_{20} + K_{02}K_{02}, \\ V^{(3)} = K_{21}K_{20} + K_{02}K_{12}, \quad V^{(4)} = K_{12}K_{10} + K_{01}K_{21}, \quad (3)$$

where K_{rs} , with $r \neq s$ indicate particle raising and lowering operators. In our numerical simulations, the particle number is set $\Omega = 40$, as a result, the Hilbert space has a dimension 861. Other parameters are $\epsilon_1 = 1.10$, $\epsilon_2 = 1.61$, $\mu_1 = 0.031$, $\mu_2 = 0.035$, $\mu_3 = 0.038$, and $\mu_4 = 0.033$. In the computation of the correlation functions, averages were taken over 50 perturbed eigenstates $|E_\alpha\rangle$ in the middle energy region.

The second model is a single-mode Dicke model [54,55], which describes the interaction between a single bosonic mode and a collection of N two-level atoms. The system can be described in terms of the collective operator $\hat{\mathbf{J}}$ for the N atoms, with

$$\hat{J}_z \equiv \sum_{i=1}^N \hat{s}_z^{(i)}, \quad \hat{J}_\pm \equiv \sum_{i=1}^N \hat{s}_\pm^{(i)}, \quad (4)$$

where $\hat{s}_{x(y,z)}^{(i)}$ are Pauli matrices divided by 2 for the i th atom. The Dicke Hamiltonian is written as [55]

$$H = \omega_0 J_z + \omega a^\dagger a + \frac{\lambda}{\sqrt{N}} (a^\dagger + a)(J_+ + J_-). \quad (5)$$

In the resonance condition, $\omega_0 = \omega$. The operators J obey the usual commutation rules for the angular momentum,

$$[J_z, J_\pm] = \pm J_\pm, \quad [J_+, J_-] = 2J_z. \quad (6)$$

We write the Hamiltonian in the form $H = H_0 + V$, with $H_0 = \omega_0 J_z + \omega a^\dagger a$. In numerical simulations, we take $N = 40$ and $\lambda = 1$, and the particle number of the bosonic field is truncated at $n = 40$.

The third model is a modified XXZ model, called a defect XXZ model [56], in which two additional magnetic fields are applied to two of the N spins in the XXZ model,

$$H = \mu_1 s_z^1 + \mu_4 s_z^4 \\ + \sum_{i=1}^{N-1} [J (s_x^i s_x^{i+1} + s_y^i s_y^{i+1}) + \mu s_z^i s_z^{i+1}]. \quad (7)$$

Without the additional magnetic fields, the system is integrable. We also write $H = H_0 + V$, where

$$H_0 = \mu_1 s_z^1 + \mu_4 s_z^4 + \sum_{i=1}^{N-1} \mu s_z^i s_z^{i+1}. \quad (8)$$

The total Hamiltonian H is commutable with S_z , the z component of the total spin, and we use the subspace with $S_z = -2$ in our numerical study. Parameters used in this model are $N = 12$, $\mu_1 = \mu_4 = 0.444$, $\mu = 0.5$, and $J = 1.4$.

The last model we employ is a modified one-dimensional (1D) Ising chain in transverse field, called a defect Ising

model [57], with the Hamiltonian

$$H = \mu_1 s_z^1 + \mu_4 s_z^4 + \sum_i^{N-1} J_z s_z^i s_z^{i+1} + \lambda \sum_{i=1}^N s_x^i. \quad (9)$$

In the form of $H = H_0 + V$,

$$H_0 = \mu_1 s_z^1 + \mu_4 s_z^4 + \sum_i^{N-1} J_z s_z^i s_z^{i+1}. \quad (10)$$

Parameters used in this model are $N = 10$, $\mu_1 = \mu_4 = 0.444$, $J_z = 1$, and $\lambda = 0.45$. The open boundary condition has been used for the last two models discussed above.

III. GENERIC DISCUSSIONS ABOUT CORRELATION FUNCTION

In this section, we discuss the type of correlation function to be studied in this paper. We use $|E_\alpha\rangle$ and $|E_i^0\rangle$ to denote eigenstates of the perturbed Hamiltonian H and of the unperturbed one H_0 , respectively,

$$H|E_\alpha\rangle = E_\alpha|E_\alpha\rangle, \quad H_0|E_i^0\rangle = E_i^0|E_i^0\rangle, \quad (11)$$

with eigenenergies in increasing order, and use V_{ij} to denote elements of the perturbation, $V_{ij} = \langle E_i^0|V|E_j^0\rangle$. We assume that the perturbation V has a sparse structure in the eigenbasis of H_0 , that is, $V_{ij} = 0$ for most of the pairs (i, j) . (All four models discussed in the previous section have this property.) We also assume that the perturbation has vanishing diagonal elements, $V_{ii} = 0$ [58]. The expansion of $|E_\alpha\rangle$ in $|E_i^0\rangle$ is written as

$$|E_\alpha\rangle = \sum_i C_{\alpha i} |E_i^0\rangle, \quad (12)$$

where the components $C_{\alpha i} = \langle E_i^0|E_\alpha\rangle$ give the EF. For the sake of simplicity in discussion, we assume that the system has the time-reversal symmetry and the elements V_{ij} , as well as the components $C_{\alpha i}$ are real.

Physically, the following transition amplitude is of interest:

$$F_{ij}(t) = \langle E_j^0|U(t)|E_i^0\rangle, \quad (13)$$

where $U(t) = e^{-iHt}$. Straightforward derivation shows that

$$F_{ij}(t) = \sum_\alpha e^{-iE_\alpha t} C_{\alpha j} C_{\alpha i}. \quad (14)$$

When the time t is not long, neighboring levels E_α give similar contributions to the phase of $e^{-iE_\alpha t}$. Suppose that the average of $C_{\alpha j} C_{\alpha i}$ over neighboring levels can be approximately treated as a smooth function of the energy E_α , denoted by $C(E_\alpha)$, which approximately holds for most EFs in quantum chaotic systems. Then,

$$F_{ij}(t) \approx \sum_\alpha e^{-iE_\alpha t} C(E_\alpha) \rightarrow \int dE e^{-iEt} C(E) \rho(E), \quad (15)$$

where $\rho(E)$ indicates the density of states. Therefore, knowledge about the function $C(E)$, which is in fact a correlation function, is useful in the study of physical quantities such as transition probabilities.

For the above-discussed reason, we study correlation functions as an average of $C_{\alpha j} C_{\alpha i}$ with respect to the energy.

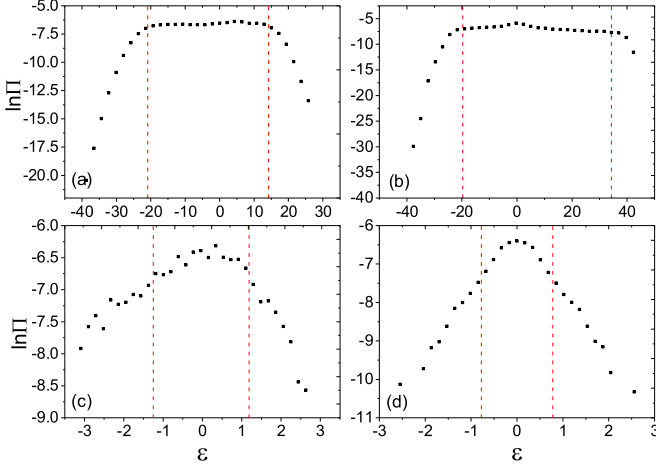


FIG. 1. Averaged shapes of EFs in the four models as functions of the energy difference ε , in the logarithmic scale. The average was taken over 50 EFs in the middle energy region in each model. The four models are (a) LMG model, (b) Dicke model, (c) defect XXZ model, and (d) defect Ising model. The vertical straight lines indicate edges of nonperturbative (NPT) regions (see the Appendix for the definition of NPT regions).

It is known that, usually, the EF of $|E_\alpha\rangle$ is approximately centered at E_α (see Fig. 1 for examples of the averaged shapes of EFs). Therefore, it is convenient to consider correlations as functions of the energy difference between perturbed and unperturbed states, namely, as functions of $\varepsilon_{\alpha l} \equiv E_l^0 - E_\alpha$. The average, which is used in the computation of the correlation functions, is taken over the perturbed energy E_α for a fixed value of ε . Determination of the label l will be specified below, when discussing specific correlation functions.

We find that correlation functions behave differently for labels i and j coupled in different ways. Therefore, we study correlation functions according to the ways of coupling. Specifically, we use S_n to denote the set of those pairs (i, j) , for each of which the two unperturbed states $|E_i^0\rangle$ and $|E_j^0\rangle$ have an “ n -step” coupling, that is,

$$S_n = \{(i, j) : (V^n)_{ij} \neq 0, (V^m)_{ij} = 0 \text{ for } 0 < m < n\}. \quad (16)$$

We call a correlation function, which is computed for pairs (i, j) belonging to a given set S_n , an n th-order correlation function.

For example, the first-order correlation function is defined by

$$C_1(\varepsilon) = \langle C_{\alpha i} C_{\alpha j} \rangle / \Pi(\varepsilon) \quad \text{for } (i, j) \in S_1, \quad (17)$$

where $\Pi(\varepsilon)$ indicates the averaged shape of the EFs, $\Pi(\varepsilon) = \langle |C_{\alpha i}|^2 \rangle$. Here and hereafter, for an average indicated by $\langle \rangle$, we take $|E_l^0\rangle = |E_i^0\rangle$ for $\varepsilon_{\alpha l}$ discussed above. The second-order correlation function is defined by

$$C_2(\varepsilon) = \langle C_{\alpha i} C_{\alpha j} \rangle' / \Pi(\varepsilon) \quad \text{for } (i, j) \in S_2, \quad (18)$$

where the prime in $\langle \rangle'$ indicates an average for which the labels l in $\varepsilon_{\alpha l}$ satisfy $V_{il} V_{lj} \neq 0$.

The average shape of the EFs, namely, $\Pi(\varepsilon)$, are plotted in Fig. 1. In both the LMG and the Dicke models, $\Pi(\varepsilon)$ has a platform in the central region, with long tails decaying

exponentially, while it is approximately exponentially localized in the defect Ising model and is partially so in the defect XXZ model. This difference is related to the fact that the Hamiltonian matrices in the two former models have a clear band structure, but those in the two latter models do not. In all four models, the main bodies of the EFs lie within the so-called nonperturbative (NPT) regions of EFs [46,59], which are predicted by a generalized Brillouin-Wigner perturbation theory [22]. Edges of the NPT regions are indicated by vertical dashed lines in Fig. 1. (See the Appendix for the definition of NPT regions of EFs.)

IV. CORRELATION FUNCTIONS FOR V_{ij} WITH HOMOGENEOUS SIGN

In this section, we discuss correlation functions for perturbations V , whose nonzero elements have a homogeneous sign.

A. First-order correlation function

To find an expression for the correlation function $C_1(\varepsilon)$, let us write the stationary Schrödinger equation, $H|E_\alpha\rangle = E_\alpha|E_\alpha\rangle$, in the form

$$C_{\alpha i} = -\frac{1}{\varepsilon_{\alpha i}} \sum_{j \in g_i} V_{ij} C_{\alpha j}, \quad (19)$$

where g_i indicates the set of those labels j for which V_{ij} are nonzero, namely,

$$g_i = \{j : V_{ij} \neq 0\}. \quad (20)$$

Multiplying both sides of Eq. (19) by $C_{\alpha i}$, then taking the average $\langle \rangle$ one gets

$$\langle |C_{\alpha i}|^2 \rangle = -\frac{1}{\varepsilon} \overline{N} \langle V_{ij} C_{\alpha i} C_{\alpha j} \rangle, \quad (21)$$

where $\overline{N} = \langle \sum_{j \in g_i} 1 \rangle$ is the average number of coupling to one unperturbed state. For quantum chaotic systems, when the fluctuations of nonzero V_{ij} are not very strong, the average over $V_{ij} C_{\alpha i} C_{\alpha j}$ can be taken separately for V_{ij} and $C_{\alpha i} C_{\alpha j}$, giving

$$\langle V_{ij} C_{\alpha i} C_{\alpha j} \rangle \simeq \overline{V} \langle C_{\alpha i} C_{\alpha j} \rangle, \quad (22)$$

where $\overline{V} = \langle V_{ij} \rangle$ for $V_{ij} \neq 0$. Then, Eq. (21) gives [60]

$$C_1(\varepsilon) \simeq -\frac{\varepsilon}{\overline{V} \overline{N}}. \quad (23)$$

An interesting feature can be seen from Eq. (23), that is, in the case that \overline{V} and \overline{N} change slowly with ε , the first-order correlation function C_1 is almost linear in ε . Thus, at ε close to 0, the two components $C_{\alpha i}$ and $C_{\alpha j}$ have almost uncorrelated signs, while, for $|\varepsilon|$ not small, $|C_1|$ can be obviously larger than zero and $C_{\alpha i} C_{\alpha j}$ tend to have the same sign as $[-\varepsilon \text{sgn}(V_{ij})]$.

Numerical simulations have been performed in the four models discussed previously to check the predictions given above. In all four models, nonzero V_{ij} have the positive sign. In the two defect spin models, nonzero elements V_{ij} share the same value, and good agreement between direct numerical simulations and the prediction of Eq. (23) has been observed in the whole regime of ε (Fig. 2).

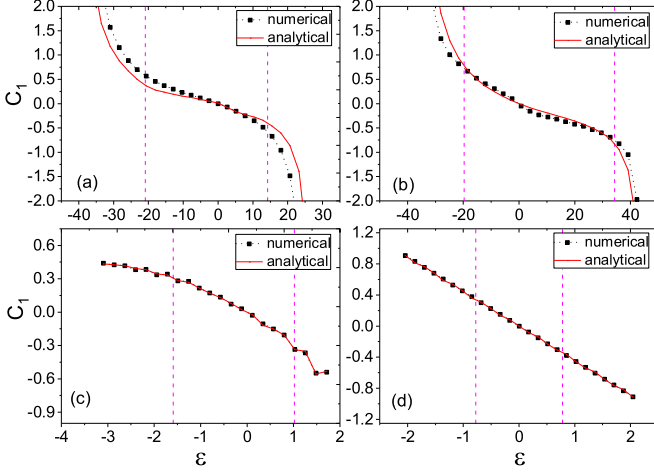


FIG. 2. The first-order correlation function C_1 in Eq. (17) for $(i, j) \in S_1$, as a function of the energy difference ε , in the four models. Solid curves indicate predictions of Eq. (23). (See Fig. 1 for the meaning of the vertical dashed lines.)

In the two models of LMG and Dicke, nonzero elements V_{ij} have fluctuations, being stronger in the LMG model. In these two models, the agreement between numerical simulations and analytical predictions is good in the central region of the EFs, but it is not so good in the long-tail regions with large $|\varepsilon|$. For comparison, we have also computed the correlation function for the set composed of all the pairs (i, j) and found that it is close to zero as predicted by the RMT, except in the long-tail regions of the EFs in which some perturbative treatments can be valid [8,22].

B. Second-order correlation function

To find an expression for the second-order correlation function, let us consider a label k , for which $V_{ik}V_{kj} \neq 0$. Making use of Eq. (19), one gets

$$|C_{\alpha k}|^2 = \frac{1}{\varepsilon_{\alpha k}^2} \sum_i |V_{ki}|^2 |C_{\alpha i}|^2 + \frac{1}{\varepsilon_{\alpha k}^2} \sum_{i \neq j} V_{ki} V_{kj} C_{\alpha i} C_{\alpha j}. \quad (24)$$

Taking the average $\langle \cdot \rangle$ on both sides of Eq. (24) and following arguments similar to those leading to Eq. (23), one gets

$$\Pi(\varepsilon) \simeq \frac{\overline{V^2}}{\varepsilon^2} \Pi_d(\varepsilon) \overline{N} + \frac{\overline{W}}{\varepsilon^2} \overline{N}(\overline{N} - 1) \langle C_{\alpha i} C_{\alpha j} \rangle', \quad (25)$$

where $\overline{V^2} = \langle V_{ij}^2 \rangle$, $\overline{W} = \langle V_{ki} V_{kj} \rangle'$, and $\Pi_d(\varepsilon) \equiv \langle |C_{\alpha i}|^2 \rangle'$. Note that $\Pi_d(\varepsilon)$ is not exactly the same as $\Pi(\varepsilon)$.

Writing $\Pi_d(\varepsilon) = \eta \Pi(\varepsilon)$, we get the following expression of C_2 :

$$C_2(\varepsilon) \simeq \frac{\varepsilon^2 - \overline{V^2} \overline{N} \eta}{\overline{W} \overline{N} (\overline{N} - 1)}, \quad (26)$$

showing a quadratic dependence on ε . According to Eq. (26), the two components $C_{\alpha i}$ and $C_{\alpha j}$ of $(i, j) \in S_2$ have a sign correlation different from that for (i, j) in the set S_1 discussed above. For example, for ε around 0, the average of $C_{\alpha i} C_{\alpha j}$ of $(i, j) \in S_2$ has a minus sign.

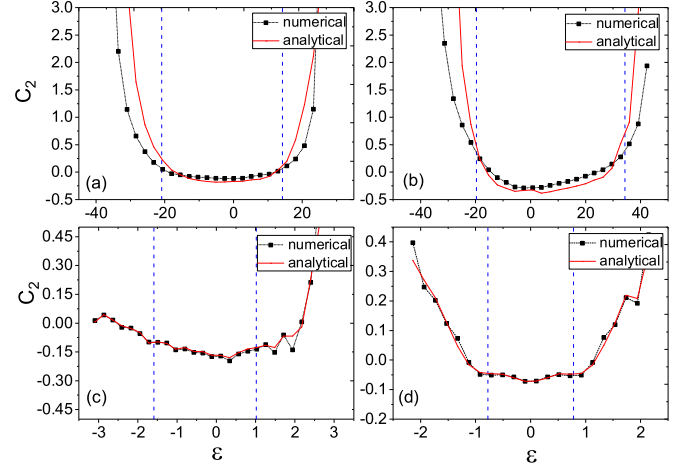


FIG. 3. Similar to Fig. 2, but for the correlation function C_2 in Eq. (18) with predictions given by Eq. (26).

Numerical tests for the prediction in Eq. (26) are shown in Fig. 3. Similar to the case of first-order correlation discussed above, in the two defect spin models, good agreement has been observed in the whole regime of ε . In the two models of LMG and Dicke, the agreement is relatively good in the central region of the EFs, but is not good in the long-tail regions with large $|\varepsilon|$.

V. CORRELATION FUNCTIONS FOR V_{ij} WITH NONHOMOGENEOUS SIGNS

In this section, we discuss the case that nonzero elements V_{ij} have both positive and negative signs. In this case, nonzero V_{ij} have quite strong fluctuations, such that Eq. (23) does not hold.

We find that sign correlation still exists among $C_{\alpha i}$ and $C_{\alpha j}$, for those unperturbed states that are coupled by the perturbation V . To see this point, let us divide the set S_1 into two subsets according to the sign of V_{ij} , denoted by S_1^\pm , respectively. We use C_1^\pm to denote the corresponding (first-order) correlation functions, defined by

$$C_1^\pm = \langle C_{\alpha i} C_{\alpha j} \rangle^\pm / \Pi(\varepsilon) \quad \text{for } (i, j) \in S_1^\pm. \quad (27)$$

Following arguments similar to those leading to Eq. (23), one gets

$$\overline{V}_+ \overline{N}_+ C_1^+ + \overline{V}_- \overline{N}_- C_1^- \simeq -\varepsilon, \quad (28)$$

where \overline{V}_\pm and \overline{N}_\pm are defined in a way similar to \overline{V} and \overline{N} discussed previously, but with respect to the sets S_1^\pm , respectively.

Let us define a correlation function weighted by the sign of V_{ij} , denoted by \tilde{C}_1 ,

$$\tilde{C}_1 = \langle \text{sgn}(V_{ij}) C_{\alpha i} C_{\alpha j} \rangle / \Pi(\varepsilon), \quad (i, j) \in S_1, \quad (29)$$

Similar to Eq. (23), it is found that

$$\tilde{C}_1(\varepsilon) \simeq -\varepsilon (|\overline{V}| \overline{N})^{-1}, \quad (30)$$

where $|\overline{V}| = \langle |V_{ij}| \rangle$.

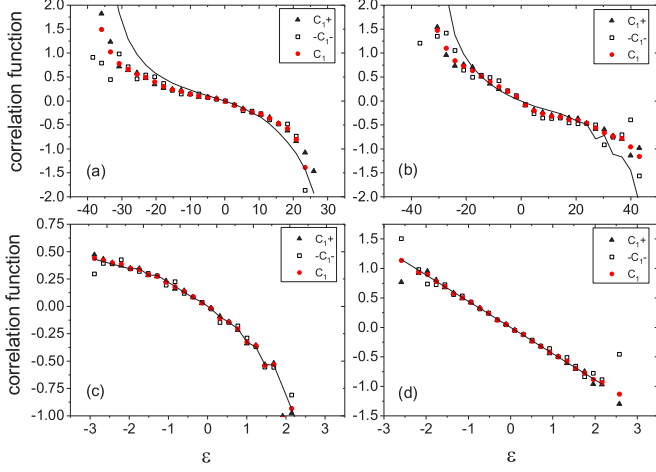


FIG. 4. Similar to Fig. 2, but for the correlation functions C_1^\pm in Eq. (27) and \tilde{C}_1 in Eq. (29) in modified versions of the four models, in which 30% of the nonzero V_{ij} are negative. The solid curves are given by the theoretical prediction on the right hand side of Eq. (30).

For the simplicity in discussion, let us consider the specific case that $\bar{V}_+ = -\bar{V}_- = |\bar{V}|$. Then, Eqs. (30) and (28) give

$$\bar{N}\tilde{C}_1 \simeq \bar{N}_+C_1^+ - N_-C_1^-. \quad (31)$$

Noting that $\bar{N}_+ + \bar{N}_- = \bar{N}$, it would be reasonable to expect that

$$\tilde{C}_1 \simeq C_1^+ \simeq -C_1^-. \quad (32)$$

This suggests that, for pairs (i, j) in the set S_1 , $C_{ai}C_{aj}$ tend to have the same sign as $[-\varepsilon \text{sgn}(V_{ij})]$. Note that this phenomenon has also been observed in the homogeneous-sign case discussed in the previous section [see Eq. (23)].

To test whether the expectation in Eq. (32) is correct, we have studied modified versions of the four models discussed above, changing the signs of a percentage of randomly chosen nonzero elements V_{ij} to the negative one. For brevity, we call the models thus obtained the random LMG model, and so on. Our numerical simulations confirm the validity of Eq. (32) in all four modified models and show that Eq. (30) works well except in the tail regions of the EFs in the LMG and the Dicke models (Fig. 4) [61]. The sign correlation between C_{ai} and C_{aj} has been observed in a direct computation of the following quantity:

$$C_{\text{sign}} = \langle \text{sgn}(C_{ai}C_{aj}) \text{sgn}(V_{ij}) \rangle_\varepsilon \quad \text{for } (i, j) \in S_1. \quad (33)$$

As seen in Fig. 5, the sign correlation increases with increasing $|\varepsilon|$.

VI. APPLICATIONS

In this section, we discuss two applications of the results obtained in previous sections. One is for a relation between some transition probabilities (Sec. VIA) and the other is for expectation values of some local observables (Sec. VIB).

A. A relation between two transition probabilities

Let us consider the transition probability from an initial state $|E_i^0\rangle$ to all those states $|E_j^0\rangle$, which are directly coupled

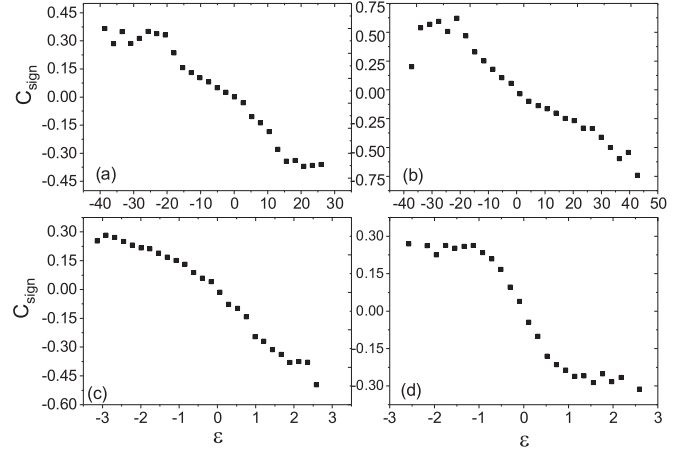


FIG. 5. Sign correlation between directly coupled components of the EFs, with C_{sign} defined in Eq. (33).

to $|E_i^0\rangle$ by the perturbation V , namely, with $V_{ij} \neq 0$. Denoting this probability by $F_i(t)$, it is written as

$$F_i(t) = \sum_{j \in g_i} |F_{ij}(t)|^2, \quad (34)$$

where F_{ij} is the transition amplitude in Eq. (13). For simplicity in discussion, we consider a case satisfying the following requirements: (i) nonzero elements V_{ij} are close to each other, (ii) the values of $|C_{aj}|$ do not have large fluctuations with respect to the label j , and (iii) the ε dependence of \bar{V} and \bar{N} can be neglected.

Let us first discuss variation of F_{ij} with j . To this end, noting that $E_\alpha = E_i^0 - \varepsilon_{ai}$, we write F_{ij} as

$$F_{ij} = \left(\sum_\alpha C_{ai}C_{aj} e^{i\varepsilon_{ai}t} \right) e^{-iE_i^0 t}. \quad (35)$$

According to Eq. (23), $C_{ai}C_{aj}$ are on average proportional to $-\varepsilon \Pi(\varepsilon)$, hence, the main contribution to F_{ij} should come from those perturbed states $|E_\alpha\rangle$ for which $|\varepsilon_{ai} \Pi(\varepsilon_{ai})|$ are large. For these perturbed states, as discussed previously, $C_{ai}C_{aj}$ tend to have the same sign as $(-\varepsilon_{ai} V_{ij})$. Noting the homogeneity of the sign of nonzero V_{ij} and the smallness of the fluctuation of $|C_{aj}|$ with j , it is seen that, on average, F_{ij} do not have large fluctuation with j for $j \in g_i$.

Then, we get the following approximation for these labels j :

$$F_{ij}(t) \simeq \frac{1}{N} \sum_{j' \in g_i} F_{ij'}(t), \quad (36)$$

and, as a result, the following expression of $F_i(t)$:

$$F_i(t) \simeq \bar{N} \left| \frac{1}{N} \sum_{j' \in g_i} F_{ij'}(t) \right|^2 = \frac{1}{N} \left| \sum_\alpha \sum_{j \in g_i} C_{ai}C_{aj} e^{i\varepsilon_{ai}t} \right|^2. \quad (37)$$

Due to the assumed small fluctuation of nonzero V_{ij} , $F_i(t)$ can be further written as $F_i(t) \simeq \frac{1}{N} \left| \frac{1}{V} \sum_\alpha \sum_{j \in g_i} V_{ij} C_{aj} C_{ai} e^{i\varepsilon_{ai}t} \right|^2$. Finally, making use of

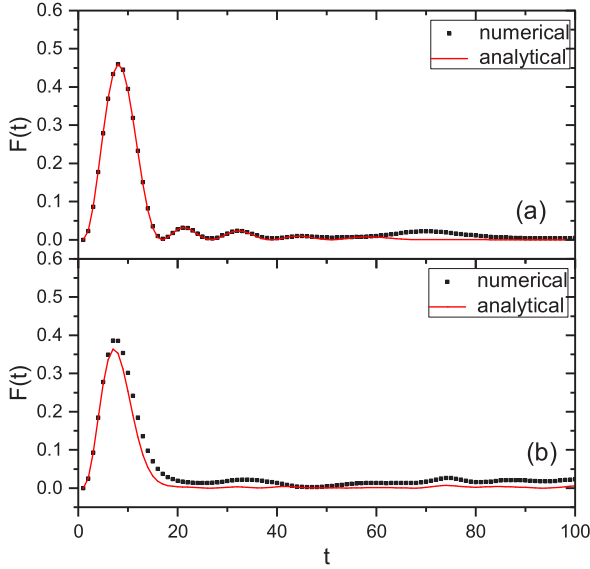


FIG. 6. Variation of the transition probability F_i in Eq. (34) (solid squares). Solid curves indicate predictions of Eq. (38). The times are given in units of $\tau = 10^{-3}\tau_H$, where $\tau_H = 1/d$ is the Heisenberg time with d the averaged level spacing. The results are for (a) Dicke model and (b) defect XXZ model.

Eq. (19), one gets the following expression,:

$$F_i(t) \simeq \frac{1}{N} \left| \frac{1}{\sqrt{V}} \sum_{\alpha} \varepsilon_{\alpha i} |C_{\alpha i}|^2 e^{i\varepsilon_{\alpha i} t} \right|^2 \simeq \frac{1}{N(V)^2} \left| \frac{\partial s_i(t)}{\partial t} \right|^2, \quad (38)$$

where $s_i(t)$ is defined by

$$s_i(t) = \langle E_i^0 | e^{-i(H-E_i^0)t} | E_i^0 \rangle. \quad (39)$$

It is easy to see that, apart from a phase factor, $s_i(t)$ gives the survival probability amplitude for the initial state.

To test numerically the prediction of Eq. (38), we consider the Dicke model and the defect XXZ model. (The LMG model and the defect Ising model do not meet the requirements discussed above.) Numerical simulations show that Eq. (38) works well in the Dicke model and works approximately in the defect XXZ model (see Fig. 6 for two examples). Examples for the survival probabilities in these two models are shown in Fig. 7.

B. Expectation values of some local observables

In another application, we consider the expectation values of s_x^i and of $s_x^i s_x^{i+1}$ in the defect Ising model, i.e., $\langle E_{\alpha} | s_x^i | E_{\alpha} \rangle$ and $\langle E_{\alpha} | s_x^i s_x^{i+1} | E_{\alpha} \rangle$. Due to the fact that s_x^i is a part of the perturbation V [see Eqs. (9) and (10)], $V = \lambda \sum_{i=1}^N s_x^i$, these expectation values can be related to the first- and second-order correlation functions given previously.

First, the quantity $\langle E_{\alpha} | s_x^i | E_{\alpha} \rangle$ can be expressed as

$$\langle E_{\alpha} | s_x^i | E_{\alpha} \rangle = \sum_{k,l} C_{\alpha k} (s_x^i)_{kl} C_{\alpha l}. \quad (40)$$

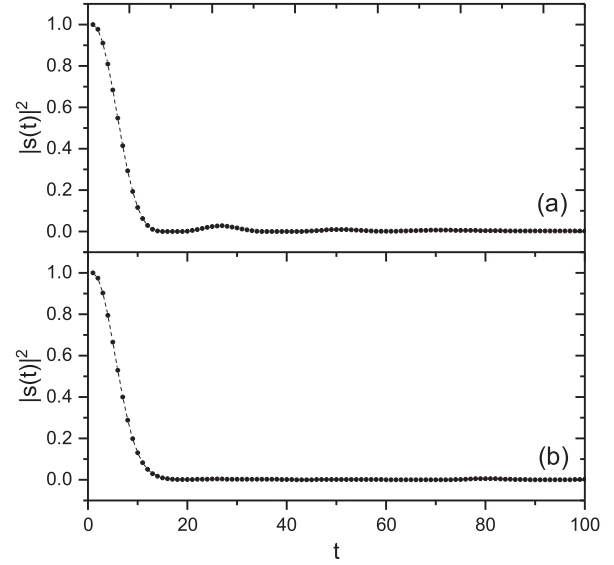


FIG. 7. Variations of the survival probability $|s(t)|^2$ under the same initial conditions as those for Fig. 6.

For each given label k , there is only one label l , denoted by l_k , for which $(s_x^i)_{kl} \neq 0$; and for these labels $(s_x^i)_{kl} = 0.5$. Then, one gets

$$\langle E_{\alpha} | s_x^i | E_{\alpha} \rangle = \frac{1}{2} \sum_k C_{\alpha k} C_{\alpha l_k} \simeq \frac{1}{2} \sum_k C_1(\varepsilon_{\alpha k}) \Pi(\varepsilon_{\alpha k}). \quad (41)$$

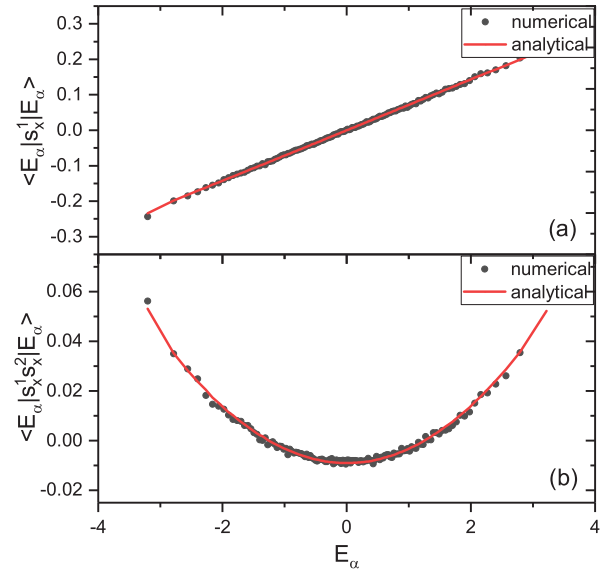


FIG. 8. Expectation values of two local operators for eigenstates $|E_{\alpha}\rangle$ in the Defect Ising model, with spin number $N = 14$. Top: Expectation values of s_x^1 (solid circles). The solid curve indicates predictions of Eq. (42). Bottom: Expectations values of $s_x^1 s_x^2$, with predictions given in Eq. (44). In the numerical simulations, each solid circle was obtained by taking average over 128 neighboring EFs.

Substituting the expression of $\mathcal{C}_1(\varepsilon)$ in Eq. (23) into Eq. (41), we get

$$\langle E_\alpha | s_x^i | E_\alpha \rangle \simeq -\frac{1}{\lambda \bar{N}} \sum_k \varepsilon_{\alpha k} \Pi(\varepsilon_{\alpha k}). \quad (42)$$

Similarly, $\langle E_\alpha | s_x^i s_x^{i+1} | E_\alpha \rangle$ can be written as

$$\begin{aligned} \langle E_\alpha | s_x^i s_x^{i+1} | E_\alpha \rangle &= \sum_{k,m,l} C_{\alpha k}(s_x^i)_{km}(s_x^{i+1})_{ml} C_{\alpha l} \\ &= \frac{1}{4} \sum_m C_{\alpha k_m} C_{\alpha l_m} \simeq \frac{1}{4} \sum_m \Pi(\varepsilon_{\alpha m}) \mathcal{C}_2(\varepsilon_{\alpha m}), \end{aligned} \quad (43)$$

where k_m and l_m indicate those values of k and l for which V_{k_m} and $V_{m l_m}$ are not equal to zero. Substituting the expression of $\mathcal{C}_2(\varepsilon)$ in Eq. (26) into Eq. (43), after some algebra, we get

$$\langle E_\alpha | s_x^i s_x^{i+1} | E_\alpha \rangle \simeq \frac{\sum_m \Pi(\varepsilon_{\alpha m}) \varepsilon_{\alpha m}^2}{\lambda^2 \bar{N} (\bar{N} - 1)} - \frac{0.25}{\bar{N} - 1}. \quad (44)$$

We have tested the predictions in Eqs. (42) and (44) numerically. As shown in Fig. 8, the numerical simulations are in good agreement with the analytical predictions.

VII. CONCLUSIONS

In summary, in this paper, we have studied correlation functions with respect to the energy difference between perturbed and unperturbed states, in quantum chaotic systems whose Hamiltonian matrices have a sparse structure in the unperturbed bases. Analytical expressions have been derived for some correlation functions and have been tested in numerical simulations performed in four models. Applications are given for transition probabilities, as well as expectation values of some local observables. It should be reasonable to expect that more applications may be found in future investigations.

ACKNOWLEDGMENTS

The authors are grateful to J. Gong for valuable discussions. This work was partially supported by the Natural Science Foundation of China under Grants No. 11275179 and No.

11535011, and the National Key Basic Research Program of China under Grant No. 2013CB921800.

APPENDIX: GENERALIZED BRILLOUIN-WIGNER PERTURBATION THEORY (GBWPT)

In this Appendix, we recall the definition of (NPT) regions of EFs [59]. Consider a Hamiltonian of the form

$$H = H_0 + V, \quad (A1)$$

where H_0 is an unperturbed Hamiltonian and V represents a generic perturbation. Eigenstates of H and H_0 are denoted by $|\alpha\rangle$ and $|k\rangle$, respectively,

$$H|\alpha\rangle = E_\alpha|\alpha\rangle, \quad H_0|k\rangle = E_k^0|k\rangle, \quad (A2)$$

with labels α and k in energy order.

As shown in a generalized Brillouin-Wigner perturbation theory [22], for each perturbed state $|\alpha\rangle$, the set of unperturbed states $|k\rangle$ is divided into two substates, denoted by S_α and \bar{S}_α . The related projection operators,

$$P_{S_\alpha} = \sum_{|k\rangle \in S_\alpha} |k\rangle \langle k|, \quad Q_{\bar{S}_\alpha} = \sum_{|k\rangle \in \bar{S}_\alpha} |k\rangle \langle k| = 1 - P_{S_\alpha}, \quad (A3)$$

divide the perturbed state into two parts, $|\alpha_s\rangle \equiv P_{S_\alpha}|\alpha\rangle$ and $|\alpha_{\bar{s}}\rangle \equiv Q_{\bar{S}_\alpha}|\alpha\rangle$. If this division satisfies the following condition:

$$\lim_{n \rightarrow \infty} \langle \phi | (T_\alpha^\dagger)^n T_\alpha^n | \phi \rangle = 0 \quad \forall |\phi\rangle, \quad (A4)$$

where

$$T_\alpha = \frac{1}{E_\alpha - H_0} Q_{\bar{S}_\alpha} \lambda V, \quad (A5)$$

then, making use of the part $|\alpha_s\rangle$, the other part $|\alpha_{\bar{s}}\rangle$ can be expanded in a convergent perturbation expansion, i.e.,

$$|\alpha_{\bar{s}}\rangle = T_\alpha |\alpha_s\rangle + T_\alpha^2 |\alpha_s\rangle + \cdots + T_\alpha^n |\alpha_s\rangle + \cdots. \quad (A6)$$

Writing S_α in the form

$$S_\alpha = \{|k\rangle : k_1 \leq k \leq k_2\}, \quad (A7)$$

the smallest set S_α that satisfies the condition (A4) is called the *nonperturbative (NPT) region* of the state $|\alpha\rangle$.

-
- [1] *Quantum Chaos: Between Order and Disorder*, edited by G. Casati and B. V. Chirikov (Cambridge University Press, Cambridge, England, 1994).
- [2] F. Haake, *Quantum Signatures of Chaos*, 3rd ed. (Springer-Verlag, Berlin, 2010).
- [3] A. D. Mirlin, *Phys. Rep.* **326**, 259 (2000).
- [4] M. V. Berry, *J. Phys. A: Math. Gen.* **10**, 2083 (1977).
- [5] V. Buch, R. B. Gerber, and M. A. Ratner, *J. Chem. Phys.* **76**, 5397 (1982).
- [6] D. C. Meredith, S. E. Koonin, and M. R. Zirnbauer, *Phys. Rev. A* **37**, 3499 (1988).
- [7] M. Srednicki, *Phys. Rev. E* **54**, 954 (1996); *J. Phys. A: Math. Gen.* **29**, 5817 (1996).

- [8] V. V. Flambaum, G. F. Gribakin, and F. M. Izrailev, *Phys. Rev. E* **53**, 5729 (1996).
- [9] P. O'Connor, J. Gehlen, and E. J. Heller, *Phys. Rev. Lett.* **58**, 1296 (1987).
- [10] S. Hortikar and M. Srednicki, *Phys. Rev. E* **57**, 7313 (1998).
- [11] A. Bäcker and R. Schubert, *J. Phys. A: Math. Gen.* **35**, 539 (2002).
- [12] J. D. Urbina and K. Richter, *J. Phys. A: Math. Gen.* **36**, L495 (2003); *Phys. Rev. E* **70**, 015201 (2004); *Phys. Rev. Lett.* **97**, 214101 (2006).
- [13] E. J. Heller, *Phys. Rev. Lett.* **53**, 1515 (1984); L. Kaplan and E. J. Heller, *Ann. Phys. (N.Y.)* **264**, 171 (1998).

- [14] W. E. Bies, L. Kaplan, M. R. Haggerty, and E. J. Heller, *Phys. Rev. E* **63**, 066214 (2001).
- [15] H. Schanz, *Phys. Rev. Lett.* **94**, 134101 (2005).
- [16] I. V. Gornyi and A. D. Mirlin, *Phys. Rev. E* **65**, 025202 (2002).
- [17] L. Kaplan, *Phys. Rev. E* **71**, 056212 (2005).
- [18] V. I. Falko and K. B. Efetov, *Phys. Rev. Lett.* **77**, 912 (1996).
- [19] M. Horvat and T. Prosen, *J. Phys. A* **36**, 4015 (2003).
- [20] Y. Alhassid and C. H. Lewenkopf, *Phys. Rev. Lett.* **75**, 3922 (1995).
- [21] V. N. Prigodin, *Phys. Rev. Lett.* **74**, 1566 (1995).
- [22] W.-G. Wang, F. M. Izrailev, and G. Casati, *Phys. Rev. E* **57**, 323 (1998).
- [23] S. Gnutzmann, J. P. Keating, and F. Pietet, *Ann. Phys.* **325**, 2595 (2010).
- [24] A. T. Ngo, E. H. Kim, and S. E. Ulloa, *Phys. Rev. B* **84**, 155457 (2011).
- [25] R. Höhmann, U. Kuhl, H. J. Stockmann, J. D. Urbina, and M. R. Dennis, *Phys. Rev. E* **79**, 016203 (2009).
- [26] A. M. Smith and L. Kaplan, *Phys. Rev. E* **80**, 035205 (2009); **82**, 016214 (2010).
- [27] Y. Alhassid, *Rev. Mod. Phys.* **72**, 895 (2000).
- [28] J. P. Bird, R. Akis, D. K. Ferry, D. Vasileska, J. Cooper, Y. Aoyagi, and T. Sugano, *Phys. Rev. Lett.* **82**, 4691 (1999).
- [29] G. Hackenbroich, C. Viviescas, B. Elattari, and F. Haake, *Phys. Rev. Lett.* **86**, 5262 (2001).
- [30] H. E. Türeci, H. G. L. Schwefel, Ph. Jacquod, and A. Douglas Stone, *Prog. Opt.* **47**, 75 (2005).
- [31] K. Schaadt, T. Guhr, C. Ellegaard, and M. Oxborrow, *Phys. Rev. E* **68**, 036205 (2003).
- [32] U. Dörr, H. J. Stockmann, M. Barth, and U. Kuhl, *Phys. Rev. Lett.* **80**, 1030 (1998).
- [33] J.-H. Yeh, J. A. Hart, E. Bradshaw, T. M. Antonsen, E. Ott, and S. M. Anlage, *Phys. Rev. E* **81**, 025201(R) (2010); **82**, 041114 (2010).
- [34] M.-J. Lee, T. M. Antonsen, and E. Ott, *Phys. Rev. E* **87**, 062906 (2013).
- [35] C. C. Chen, Y. T. Yu, R. C. C. Chen, Y. J. Huang, K. W. Su, Y. F. Chen, and K. F. Huang, *Phys. Rev. Lett.* **102**, 044101 (2009).
- [36] V. Zelevinsky, B. A. Brown, N. Frazier, and M. Horoi, *Phys. Rep.* **276**, 85 (1996).
- [37] Y. L. Bolotin, V. Y. Gonchar, and V. N. Tarasov, *Phys. Atom. Nuclei* **58**, 1499 (1995).
- [38] H. Olofsson, S. Aberg, O. Bohigas, and P. Leboeuf, *Phys. Rev. Lett.* **96**, 042502 (2006).
- [39] J. M. Deutsch, *Phys. Rev. A* **43**, 2046 (1991).
- [40] M. Srednicki, *Phys. Rev. E* **50**, 888 (1994).
- [41] M. Rigol, V. Dunjko, and M. Olshanii, *Nature (London)* **452**, 854 (2008).
- [42] A. Altland and F. Haake, *Phys. Rev. Lett.* **108**, 073601 (2012).
- [43] L. F. Santos, F. Borgonovi, and F. M. Izrailev, *Phys. Rev. Lett.* **108**, 094102 (2012).
- [44] S. Müller, S. Heusler, P. Braun, F. Haake, and A. Altland, *Phys. Rev. Lett.* **93**, 014103 (2004), and references therein.
- [45] T. Gorin, T. Prosen, T. H. Seligman, and M. Žnidarič, *Phys. Rep.* **435**, 33 (2006).
- [46] W.-G. Wang, *Phys. Rev. E* **65**, 036219 (2002).
- [47] J. Wang and W.-g. Wang, *Chaos, Solitons Fractals* **91**, 291 (2016).
- [48] J. B. French and S. S. M. Wong, *Phys. Lett. B* **33**, 449 (1971).
- [49] L. Benet and H. A. Weidenmueller, *J. Phys. A* **36**, 3569 (2003).
- [50] M. Vyas, V. K. B. Kota, and N. D. Chavda, *Phys. Rev. E* **81**, 036212 (2010).
- [51] T. Guhr, A. Müller-Groeling, and H. A. Weidenmüller, *Phys. Rep.* **299**, 189 (1998).
- [52] C. Pineda, T. Prosen, and E. Villaseñor, *New J. Phys.* **16**, 123044 (2014).
- [53] H. J. Lipkin, N. Meshkov, and A. J. Glick, *Nucl. Phys.* **62**, 188 (1965).
- [54] R. H. Dicke, *Phys. Rev.* **93**, 99 (1954).
- [55] C. Emary and T. Brandes, *Phys. Rev. E* **67**, 066203 (2003).
- [56] E. J. Torres-Herrera and L. F. Santos, *Phys. Rev. E* **89**, 062110 (2014).
- [57] S. O. Skrøvseth, *Europhys. Lett.* **76**, 1179 (2006).
- [58] In the case that some of the V_{ii} are nonzero, one may move $\sum_i |E_i^0\rangle V_{ii} \langle E_i^0|$ to the unperturbed Hamiltonian, with the total Hamiltonian unchanged.
- [59] W.-G. Wang, *Phys. Rev. E* **61**, 952 (2000); **65**, 066207 (2002).
- [60] A remark: The expression of \mathcal{C}_1 given here and that of \mathcal{C}_2 given in Eq. (26) are nonperturbative results.
- [61] Large fluctuations of \mathcal{C}_1^- at the largest and smallest values of ε in Fig. 4 are due to smallness of the number of the items, which are available for taking the average.